

ANOMALOUS TOTAL ENERGY DISTRIBUTION FOR A TUNGSTEN FIELD EMITTER*

L. W. Swanson and L. C. Crouser

Field Emission Corporation, McMinnville, Oregon
(Received 27 December 1965)

From a variety of electronic solid-state measurements¹⁻⁵ and theoretical analyses^{6,7} of Group-VI metals, and more particularly tungsten, it is now apparent that free-electron behavior is not manifested, nor expected. Although exact details of the band structure and Fermi-surface shape for tungsten must await further investigation, several important features are now established. Most interesting of these is an octahedral "jacklike" electron Fermi surface centered at the origin of the Brillouin zone Γ , pointed along the six $\langle 100 \rangle$ directions ($\overline{\Gamma H}$) and separated from a similarly shaped hole octahedron at symmetry points H by small "ball-like" protrusions of electron surface also centered on the $\overline{\Gamma H}$ axes; depending on the degree of spin-orbit coupling the ball-like protrusions along ΓH may also contain smaller "lens shaped" electron surfaces.^{8,9} In addition, a smaller nearly spherical hole surface is expected to occur along the $\langle 110 \rangle$ directions centered on symmetry points N .

Despite the expected non-free-electron behavior of conduction electrons in tungsten, the Hartree-Sommerfeld free-electron model has been used with apparent success to describe all heretofore measured vacuum field electron emission processes in tungsten. Among these measurements, that of the energy-distribution spectrum of field-emitted electrons provides the most direct method of elucidating possible band-structure effects that are sufficient in

magnitude to alter the emission appreciably from that expected on free-electron considerations. Total energy-distribution measurements reported^{10,11} thus far for a few specific crystallographic directions of the emitting surface (not including $\langle 100 \rangle$) have been adequately described by contemporary field-emission theory based on the free-electron model. While the work reported here agrees with previous results, it also reveals marked departures from the free-electron model for at least one surface direction, namely the $\langle 100 \rangle$.

The field-emission current density $J(\epsilon)$ per unit total energy ϵ (relative to the Fermi level $\epsilon = E - E_F$), originally derived by Young¹² for a free-electron model, can be rewritten in the following form¹³:

$$J(\epsilon) = \frac{J_0}{d} \left[\frac{e^{\epsilon/d}}{1 + e^{\epsilon/pd}} \right], \quad (1)$$

where J_0 is the 0°K current density and the dimensionless parameter p is kT/d . The parameter d (related to the rate of change of barrier tunneling probability with ϵ) is given by

$$d = \hbar e F / 2(2m\varphi)^{1/2} t(y), \quad (2)$$

where F is the applied field, φ the work function, and $t(y)$ is a slowly varying tabulated¹⁴ function of $y = (e^3 F)^{1/2} / \varphi$. The shape of the total energy-distribution function given by Eq. (1) is therefore governed only by the parameter

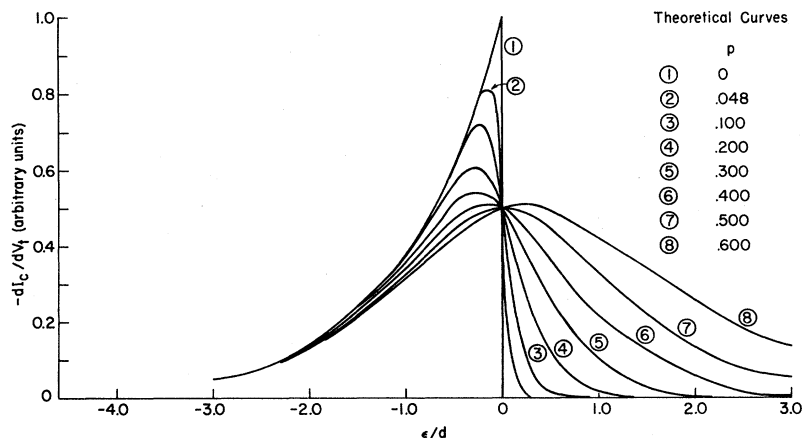


FIG. 1. Theoretical total energy-distribution plots based on the free-electron model [Eq. (1)] at various values of p .

p when, as shown in Fig. 1, $J(\epsilon)$ is plotted versus ϵ/d for various values of p . The numerator $e^{\epsilon/d}$ in Eq. (1) arises from the WKB transmission probability approximation and causes the exponential decrease in $J(\epsilon)$ for $\epsilon < 0$. Accordingly, total energy-distribution measurements over the range of p for which Eq. (1) is valid (i.e., $0 \leq p < 0.66$) are limited in practice to energy surfaces only a few tenths eV on either side of E_F .

More recently, Stratton¹⁵ has derived the total energy-distribution expression for a degenerate metal with arbitrary band structure. Assuming only specular transmission (i.e., electron transverse energy conserved during tunneling) and the usual WKB transmission approximation expanded about E_F , Stratton obtains

$$J(\epsilon) = \frac{J_0}{d} f(\epsilon) e^{\epsilon/d} \left[1 - \frac{1}{2\pi} \int_0^{2\pi} \exp(-E_m/d) d\phi_p \right], \quad (3)$$

where $f(\epsilon)$ is the electron distribution function and E_m is the maximum value of E_{yz} perpendicular to the emission direction x for a specified energy surface ϵ and polar angle ϕ_p in the yz plane. It is noted that Eq. (3) reduces to Eq. (1) when $f(\epsilon)$ is replaced by the Fermi-Dirac distribution function and the condition $E_m/d \gg 1$ is satisfied. Thus, band-structure effects appear only when the integral in Eq. (3) contributes significantly. For practical field-emission conditions $d = 0.1$ to 0.2 eV, so that shadows of constant-energy surfaces projected on a plane perpendicular to the x direction must be sufficiently small to make $E_m \leq 0.2$ eV in order for the integral of Eq. (3) to con-

tribute significantly. For degenerate metals whose Fermi surface is large and not highly curved, $E_m/d \gg 1$ and Eq. (1) is expected to describe adequately the total energy distribution of the field-emitted electrons.

We have recently measured the total energy distribution of field-emitted electrons, utilizing an improved retarding-potential energy analyzer designed by van Oostrom, for the $\langle 112 \rangle$, $\langle 116 \rangle$, $\langle 110 \rangle$, $\langle 111 \rangle$, $\langle 130 \rangle$, and $\langle 100 \rangle$ directions of atomically clean tungsten single crystals, and over a range of fields [$(3.0$ to $4.3) \times 10^7$ V/cm] and of temperatures (77 to 900°K). In agreement with earlier low-temperature measurements,^{10,11} Eq. (1) is found to describe our results adequately along all directions investigated except the $\langle 100 \rangle$ direction. The results for this direction are shown in Fig. 2, where $J(\epsilon)$ is derived from the rate of change of the collected current I_C with emitter bias voltage V_t , by the relation

$$J(\epsilon) = -(1/n) dI_C/dV_t. \quad (4)$$

The normalization factor n was adjusted to cause the experimental peak height to match theory at $p = 0.25$, and was further adjusted slightly with temperature to cause the trailing edges of the distributions to coincide for various values of p .

Comparing Figs. 1 and 2 shows that, whereas the variation of peak height, the position of peak height on the ϵ/d axis, and the shape of the leading edge (Boltzman tail) at various values of p all are in reasonable agreement with theory, a broad unexpected shoulder oc-

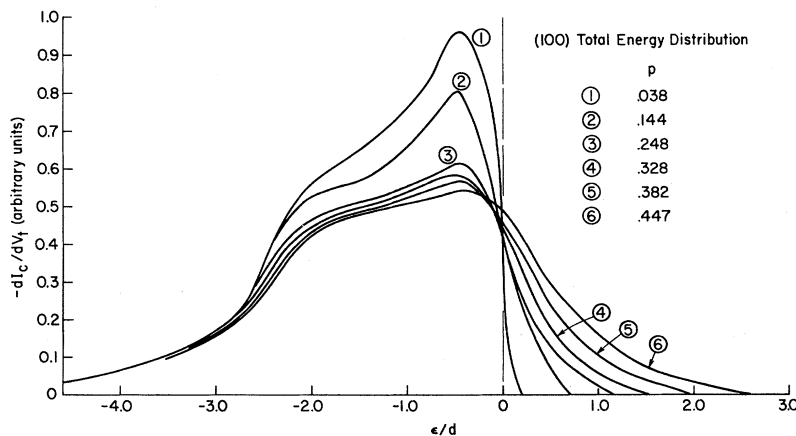


FIG. 2. Experimental total energy-distribution plots along the $\langle 100 \rangle$ direction of a tungsten field emitter as a function of p , where $d = 0.174$ eV and $F = 4.08 \times 10^7$ V/cm. At $p = 0.038$ the emitter temperature is 77°K.

curs approximately 0.35 eV below E_F on the trailing edge of the distribution. This special behavior for the $\langle 100 \rangle$ direction has been observed on both $\langle 100 \rangle$ - and $\langle 130 \rangle$ -oriented emitters employing magnetic deflection to scan various planes including the $\{100\}$. In addition, two different collector electrode surfaces provided identical results for all directions including the $\langle 100 \rangle$ direction. Thus, electron optical effects, magnetic field interactions, and collector patch effects may be discarded as possible artifacts leading to the observed $\langle 100 \rangle$ results. It should be mentioned that the direction of emission must coincide almost exactly with the $\langle 100 \rangle$ direction in order to observe the special distribution given in Fig. 2. For example, nearly complete agreement with Eq. (1) was observed along the $\langle 116 \rangle$ direction, i.e., only 13° from the $\langle 100 \rangle$ direction.

The above-mentioned anomaly in the experimental $\langle 100 \rangle$ energy distribution suggests the possibility of unusually small closed energy surfaces near E_F along the $\bar{\Gamma}\bar{H}$ direction. In order to provide a quantitative basis for this possibility, it is necessary to solve the integral in the band-structure term

$$\left[1 - \frac{1}{2\pi} \int_0^{2\pi} \exp(-E_m/d) d\phi_p \right]$$

for the various electronic energy surfaces contributing to the emission. At the present time the complexities of the proposed shapes of the energy surfaces and uncertainties as to the magnitude and variation of E_m with ϵ preclude quantitative evaluation of this term. However, certain qualitative features of the energy-surface structure can be ascertained from the variations in the band-structure term and, more specifically, E_m required to account for the results shown in Fig. 2.

At E_F (i.e., $\epsilon/d = 0$) the band-structure term must be near unity since the variation with temperature of the peak heights and their position on the ϵ/d axis are in reasonable accord with Eq. (1) and its graphical analysis in Fig. 1. This can only occur if $E_m \gg d$ for all energy surfaces near E_F . Below $\epsilon/d \cong -2.0$ the value of E_m for one of the energy surfaces contributing to the emission apparently decreases with decreasing ϵ , thus causing the band-structure term and therefore $J(\epsilon)$ to decrease sharply. On the other hand, along all other crystal directions energy surfaces contributing to the

emission must possess values of E_m that are sufficiently large to cause the band-structure term to remain near unity and independent of ϵ , at least near E_F .

On the basis of these considerations, one may list some qualitative features of the band structure along the $\langle 100 \rangle$ direction as suggested by the field-emission results. First, the energy surfaces exhibiting small values of E_m appear to be closed surfaces centered on the $\bar{\Gamma}\bar{H}$ axis with the Fermi surface subtending an angle from the center of the zone Γ not exceeding 26° . Second, these energy surfaces become small and perhaps disappear at $\epsilon/d < -2.5$ (or alternatively $\epsilon < -0.44$ eV since $d = 0.174$ eV in this work). Finally, if the energy surfaces possessing smaller values of E_m disappear at $\epsilon < -0.44$ eV, emission must continue at lower values of ϵ from other surfaces possessing larger values of E_m . We therefore conclude that at least two separate sets of energy surfaces contribute to $J(\epsilon)$.

These experimental conclusions are in general accord with the existing ideas of the Fermi surface of tungsten as described earlier. For example, one may speculate that the small lens-shaped electron pocket^{8,9} along $\bar{\Gamma}\bar{H}$, formed by the crossing of energy bands Δ_2 and Δ_2' about 0.5 to 0.6 eV below E_F , is the primary contributor to the anomalous shoulder observed in Fig. 2; if E_m for the electron pocket disappears or becomes vanishingly small for $\epsilon < 0.4$ eV, emission will continue to be observed from the larger "jack"-shaped electron surface centered on Γ , as suggested by the Fig. 2 results. There is currently some speculation⁹ as to the actual presence of such electron pockets due to spin-orbit coupling. If our interpretation is correct, we have evidence that the small electron pockets do exist, at least near the physical surface, and extend roughly 0.4 eV below E_F .

It should be mentioned that the degree of correlation between the two Fermi-surface shapes inferred from bulk electronic measurements and theoretical considerations and from energy-distribution results is not completely clear at this time. This uncertainty arises from the unknown influence of the nearby physical surface on the interatomic potentials and, hence, on the band structure along a specific direction normal to the surface. The presence on the tungsten substrate of adsorbed atoms or molecules of a markedly different character (e.g.,

highly electronegative) may further alter band-structure calculations for Brillouin cells near the surface. Some indication of the perturbation of the band-structure term in Eq. (3) by adsorption may be derived from an investigation currently in progress of the effect of adsorbed layers on the $\langle 100 \rangle$ energy-distribution results. Also, it is hoped that a comparison of the tungsten results with similar results currently being obtained from molybdenum will shed further light on the relationships between field-emission energy-distribution spectra and band structure.

In summary, the experimental results described herein provide for the first time evidence that field emission may in special cases provide insight as to the shapes of energy surfaces near the Fermi level and near the physical surface of metals.

*Work supported by the National Aeronautics and Space Administration, Headquarters, Washington, D. C.

¹E. Fawcett and D. Griffiths, *J. Phys. Chem. Solids*

23, 1631 (1962).

²E. Fawcett and W. A. Reed, *Phys. Rev.* **134**, A723 (1964).

³J. A. Rayne, *Phys. Rev.* **133**, A1104 (1964).

⁴G. B. Brandt and J. A. Rayne, *Phys. Rev.* **132**, 1945 (1963).

⁵W. M. Walsh, Jr., and C. C. Grimes, *Phys. Rev. Letters* **13**, 523 (1964).

⁶M. F. Manning and M. I. Chodorow, *Phys. Rev.* **56**, 787 (1939).

⁷W. M. Lomer, *Proc. Phys. Soc. (London)* **80**, 489 (1962).

⁸W. M. Lomer, *Proc. Phys. Soc. (London)* **84**, 327 (1964).

⁹L. F. Mattheiss, *Phys. Rev.* **139**, A1893 (1965).

¹⁰R. D. Young and E. W. Müller, *Phys. Rev.* **113**, 115 (1959).

¹¹A. van Oostrom, thesis, University of Amsterdam, 1965 (unpublished).

¹²R. D. Young, *Phys. Rev.* **113**, 110 (1959).

¹³F. M. Charbonnier, Final Report, National Science Foundation Grant No. G-7598, 1962 (unpublished).

¹⁴R. H. Good and E. W. Müller, *Handbuch der Physik* **21**, 176 (1956).

¹⁵R. Stratton, *Phys. Rev.* **135**, A794 (1964).

PHOTOELECTRIC ION EMISSION FROM CESIATED SURFACES*

O. P. Breaux and G. Medicus

Electronic Research Branch, Air Force Avionics Laboratory, Wright-Patterson Air Force Base, Ohio

(Received 28 January 1966)

Photoelectric ion emission does not seem to have been observed at room temperature thus far. The experiments described here seem to indicate such an effect, at least for cesiated surfaces.

Apparatus.—Figure 1 shows side and front view of the tube used for detecting photoelectric ion emission. Two coaxial wire-mesh electrodes are supported by an inner and an outer wall of the Pyrex tube which is re-entrant like a Dewar vessel. The leads to the electrodes are sealed into protrusions which can be heat taped to improve the insulation between the electrodes. A ring-shaped protrusion on the other end of the tube can also be heat taped for the same purpose. A cesium reservoir at room temperature attached to the tube delivers cesium vapor of pressure $\approx 10^{-6}$ Torr. A coaxial magnetic field is furnished by two coaxial coils. Two coaxial ring-shaped fluorescent tubes were used as light sources. A sweep supply (potential V_S) furnishes electrode potential plus potential across R_P (current-sensing resistor for an X - Y plotter circuit). R_L symbolizes the

electrode leakage.

Theory.—The motion of carriers in the electric and magnetic field between the cylindrical electrodes in the collisionless case is determined by the conservation of momentum and energy. The following equations describe the projection of the trajectories on the r - ϕ plane which is perpendicular to the tube axis¹:

$$\ddot{r} - r\dot{\phi}^2 = (q/m)(-\partial V/\partial r + r\dot{\phi}B), \quad (1)$$

$$2\dot{r}\dot{\phi} + r\ddot{\phi} = -(q/m)\dot{r}B, \quad (2)$$

$$\frac{1}{2}m[\dot{r}_0^2 + (r_0\dot{\phi}_0)^2] + qV = \frac{1}{2}m[\dot{r}^2 + (r\dot{\phi})^2]. \quad (3)$$

Here q is the charge of the carriers ($q = +e$ for the ions, $q = -e$ for the electrons), m is their mass ($m = m_i$ for the ions, $m = m_e$ for the electrons); r is the radial distance of the carrier from the axis, \dot{r} is the radial velocity, $r\dot{\phi}$ is the tangential velocity; $-\partial V/\partial r$ is the radial electric field strength; B ($\approx \text{const}$) is the axial magnetic-field flux density; \dot{r}_0 is the radial ejection (initial) velocity of a carrier starting from an electrode; $r_0\dot{\phi}_0$ is its tangential ejection